Biophysical Chemistry, 31 (1988) 231–245
Elsevier

BPC 01272

The interaction of δ-hemolysin with calmodulin

Louise Garone [a], John E. Fitton [b] and Robert F. Steiner [a]

[a] *Department of Chemistry, University of Maryland at Baltimore, Baltimore, MD 21228, U.S.A. and* [b] *Pharmaceutical Division, Imperial Chemical Industries, Mereside Alderley Park, Macclesfield, U.K.*

Received 30 March 1988
Revised manuscript received 22 April 1988
Accepted 22 April 1988

δ-Hemolysin; Calmodulin; Fluorescence intensity; Fluorescence anisotropy; Tryptophan

δ-Hemolysin forms a 1:1 complex with Ca^{2+}-liganded calmodulin. Probably because of the pronounced tendency of δ-hemolysin to self-associate, the apparent binding affinity is much less than that for melittin. Complex formation is reflected by an increase in quantum yield of Trp-15 of δ-hemolysin and by increased shielding from acrylamide quenching. There is, however, no indication of a change in peptide molecular ellipticity. The binding of 2-toluidinyl-naphthalene-6-sulfonate is reduced by complex formation, suggesting the involvement of a hydrophobic region. Complex formation also blocks the proteolysis by trypsin of the bond between residues 77 and 78. The time decays of fluorescence intensity and anisotropy for tryptophan are multiexponential for both free and complexed δ-hemolysin; the average decay time for intensity is substantially increased for the complex. The localized mobility of tryptophan is greatly reduced in the complex. Complex formation appears to involve both the C-terminal lobe and the connecting strand of calmodulin.

1. Introduction

Delta toxin, or δ-hemolysin, is a protein exotoxin produced by *Staphylococcus aureus*. Williams and Harper [1] were the first to establish the existence of δ-toxin; they did so by showing that an *S. aureus* culture supernatant from which the known hemolysins had been removed still retained significant hemolytic activity. Methods have been developed for the isolation of pure δ-hemolysin which are based upon solvent extraction and hydrophobic chromatography [2–5]. Fitton et al. [5] have determined the primary structure of the basic molecular unit, which consists of 26 amino acids with the following sequence:

fM-A-Q-D-I-I-S-T-I-G-D-L-V-K-W-I-I-D-T-V-N-K-F-T-K-K

In aqueous solution δ-hemolysin exists as large molecular aggregates of molecular weight $1-2 \times 10^5$ [6–8]. In the presence of high levels of guanidine hydrochloride or detergents, the molecular weight falls to 10^4 or less, although dissociation to monomer units is incomplete even under these denaturing conditions [6–8]. It is of interest that δ-hemolysins from *S. aureus* strains isolated from canine and human hosts are similar in size and properties, despite the occurrence of nine amino acid substitutions [9–11].

Although Chou-Fasman calculations for δ-hemolysin indicate a high β-sheet potential, the existing evidence favors an α-helical conformation in aqueous solution [7,10–12]. If the amino acid sequence of the monomer is plotted as a helical wheel, it is apparent that the δ-hemolysin helix has an amphipathic nature, with a separation of polar and nonpolar faces [10,11]. The mutual con-

Correspondence address: L. Garone, Department of Chemistry, University of Maryland at Baltimore, Baltimore, MD 21228, U.S.A.

Abbreviations; TNS, 2,6-toluidinylnaphthalenesulfonate; HPLC, high-performance liquid chromatography; Mops, 3-(*N*-morpholino)propanesulfonate; CaM, calmodulin.

tact of hydrophobic groups in the nonpolar faces provides an obvious mechanism for the stabilization of aggregates of the basic monomer unit.

In recent years a number of small polypeptides have been shown to form complexes with calmodulin, the ubiquitous Ca^{2+}-binding regulatory protein of eukaryotes. These polypeptides have been viewed as models for the calmodulin-binding domains of proteins with calmodulin-regulated functions [13–18], with the expectation that these studies will identify a limited number of calmodulin-recognizing sequences and provide insight into the interaction of calmodulin with regulated proteins containing model-homologous domains. Cox et al. [17] observed that δ-hemolysin binds to Ca^{2+}-liganded calmodulin, as reflected by a blue shift and increase in intensity of the tryptophan fluorescence of the former. δ-Hemolysin is thus a potential calmodulin-binding domain model.

The present paper confirms the existence of an interaction between δ-hemolysin and Ca^{2+}-liganded calmodulin and presents further results which extend the characterization of the interaction.

2. Materials and methods

2.1. Materials

Calmodulin was isolated from bull testes (Pel Freez) by a method which involves ion-exchange chromatography on DEAE-cellulose (Whatman DE-52) and phenyl-Sepharose affinity chromatography [19]. The purity of the preparations employed was evaluated spectrophotometrically, fluorimetrically and by SDS-polyacrylamide gel electrophoresis [20]. δ-Toxin was purified as previously described [5]. Chromatographic supplies and reagents were of the highest grade available and were obtained from Sigma unless otherwise indicated.

All absorption spectra were recorded on a Cary model 219 spectrophotometer (Varian). Concentrations of native proteins were determined spectrophotometrically using a $\epsilon^{1\%}_{276}$ value of 1.8 for Ca^{2+}-saturated calmodulin ($M_r = 16\,700$) and $\epsilon^{M}_{280} = 5500$ for δ-hemolysin ($M_r = 26 \times 113 = 2938$). The concentration of nitrotyrosine-derivatized calmodulin was measured radiometrically by doping the native starting material with ^{3}H-labelled calmodulin (< 1% by mass); counting efficiencies before and after nitrotyrosine derivatization were the same.

Radiolabelled calmodulin was prepared by a modification of the reductive methylation method [21]. In a typical preparation, 1 ml of 158 μM calmodulin, in 50 mM Hepes (pH 7.5), was reacted with 6.7 μmol ^{3}HCHO (N.E.N., 75 mCi/mmol) in the presence of 3.8 μmol sodium cyanoborohydride at room temperature for 25 h. Unreacted formaldehyde and catalyst were removed by passing twice over 14 × 1.4 cm Sephadex G-25 columns, equilibrated and eluted with 50 mM Hepes (pH 7.5). The ultraviolet absorption of tyrosine in this particular radiolabelled product indicated a chemical concentration of 0.6 mg calmodulin per ml and liquid scintillation (Packard Tri-Carb 4000) counting revealed a specific activity of 6300 cpm/μg.

Preferential nitration of Tyr-99 or Tyr-138 in calmodulin was accomplished as previously described [22]. For doubly nitrated calmodulin, tetranitromethane (TNM) stock (0.836 M) was prepared by adding 0.1 ml TNM (density = 1.638 g/cm^3) to 0.9 ml of 95% ethanol. A sufficient quantity of this stock was added to calmodulin (in 50 mM Tris (pH 6.9) containing 3 mM $CaCl_2$ and 1 M NaCl) to give a concentration ratio of 250 TNM : 1 CaM. After incubation at room temperature for 24 h, the derivatized calmodulin was isolated using a short (14 × 1.4 cm) Sephadex G-25 column eluted with 50 mM Mops (pH 6.5). The concentration of nitrotyrosine in each derivative was determined from the absorption at its isosbestic wavelength (381 nm, $\epsilon^{M}_{381} = 2200$).

The extent of nitration is the average number of nitrotyrosine residues per calmodulin molecule. For a particular preparation of nitrotyrosine-derivatized calmodulin the extent of nitration can be determined in at least three ways: from the ratio of the spectrophotometric concentration of nitrotyrosine to the radiometric concentration of calmodulin; from the A_{381}/A_{276} ratio; and from the results of an amino acid analysis. Based on

applying all three methods to the same nitrotyrosine preparation, and analyzing variations among the calculated extents of nitration, the probable error in the extent of nitration calculated by any one of the three methods is 10–15% of the calculated value.

Preparative and analytical trypsin digestions were performed, the former to generate calmodulin fragments for use in binding studies, and the latter to determine the effect of various treatments on calmodulin's trypsin susceptibility. Trypsin (TRTPCK lot 35N7941, Cooper Biomedical) stock solution (~ 1 mg/ml) was prepared in distilled water and its concentration determined spectrophotometrically using $\epsilon_{280}^{1\%} = 14.18$; soybean trypsin inhibitor (type 1-S, Sigma no. T9003 lot 114F-8005) stock was similarly prepared and quantitated using $\epsilon_{280}^{1\%} = 10.0$.

2.2. Trypsin digestion

For limited trypsin digestion calmodulin was dissolved in 50 mM Hepes (pH 7.5) containing 1 mM $CaCl_2$. Trypsin stock was added to calmodulin to give a trypsin/calmodulin ratio of 1 : 400 (w/w). The reaction mixture (~ 200 μl) was incubated for 1 h at room temperature and then the reaction stopped by adding an amount of trypsin inhibitor equal in mole ratio to 4-times the amount of trypsin present. The digestion products were fractionated by reversed-phase HPLC on an analytical 25 × 0.4 cm C-18 column using a Perkin Elmer LC400 chromatograph, LC 95 detector and LC 100 computing integrator. The column was eluted with linear gradients from 7.5 to 50% acetonitrile in 10 mM Tris (pH 7.2) containing 1 mM EGTA. The TR_1C and TR_2C fractions from a number of runs were pooled and lyophilized. After resuspension the fragments' concentrations were determined spectrophotometrically [23] and aliquots were analyzed for amino acid composition. The amino acid compositions of TR_1C and TR_2C isolated by the method outlined above correspond satisfactorily to the compositions of those species predicted from the amino acid sequence of calmodulin [24]. Analytical digestions were performed in 50 mM Mops (pH 6.5) containing 1 mM $CaCl_2$. In such experiments the trypsin concentration was 0.87 μM. Inhibitor was added at the end of incubation, as mentioned previously, and the digestion products were analyzed by 12.5% polyacrylamide gel electrophoresis in the presence of 4 M urea and 2 mM EGTA [18].

2.3. Static fluorescence

δ-Hemolysin contains a single tryptophan group (Trp-15) as its sole aromatic fluorophore, while calmodulin contains two tyrosines (Tyr-99 and Tyr-138), but no tryptophan. Thus, by irradiation at wavelengths greater than or equal to 295 nm, it is possible to excite differentially the tryptophan of δ-hemolysin and examine its properties as a function of conditions.

Static fluorescence intensity measurements at a single wavelength were made using a Jasco XP-4 spectrofluorometer. Complete emission spectra were obtained using an SLM 8000C single-photon counting spectrofluorometer. In fluorescence titrations of δ-hemolysin with calmodulin, the excitation and emission wavelengths were 305 and 341 nm, respectively.

While the fluorescence intensity of δ-hemolysin in the presence of excess calmodulin was stable for periods of 1 h or more, that of free δ-hemolysin showed a slow decrease with time (~ 15% in 0.5 h), presumably because of photodecomposition. (Siliconizing the cuvette did not alleviate this loss.) To minimize errors from this source, titrations of δ-hemolysin with calmodulin were performed as a series of independent titrations of short (< 0.5 h) duration, whose ranges of calmodulin concentrations overlapped. Data from the sets of overlapping titrations were pooled and analyzed. The fluorescence intensities were corrected for dilution and for background emission.

Titrations of this kind revealed a progressive enhancement of the tryptophan fluorescence of δ-hemolysin upon addition of calmodulin. Apparent values of the equilibrium constant, K_A, for the combination (assuming a 1 : 1 stoichiometry) were computed from the relations:

$$x/(1-x) = K_A[\mathrm{CaM}] \quad (1)$$

$$x = (i-1)/(i_\infty - 1) \quad (2)$$

where x is the mole fraction of δ-hemolysin which is combined with calmodulin, i the fluorescence intensity relative to that of free δ-hemolysin for a particular level of calmodulin, i_∞ the limiting relative intensity at a large excess of calmodulin, and [CaM] the concentration of uncombined calmodulin. The values of i_∞ were obtained by double-reciprocal extrapolation of i^{-1} vs. the reciprocal of the total calmodulin concentration ($[\text{CaM}]_t^{-1}$) to $[\text{CaM}]_t^{-1} = 0$. The values of i_∞ were used to compute x as a function of [CaM]. Values of K_A were computed from the linear regression of $x/(1-x)$ vs. [CaM] [25].

The dynamic quenching of Trp-15 by acrylamide was measured in the absence and presence of calmodulin and analyzed by standard procedures to obtain the second-order rate constants for quenching [26,27]. In the range of acrylamide concentrations studied, 0–0.15 M, such data were well-fitted by straight lines. Slopes of the fitted lines, the Stern-Volmer constants, were combined with the average fluorescence lifetimes in the absence and presence of calmodulin to calculate the respective second-order rate constants for quenching [26,27].

2.4. Circular dichroism

Near-ultraviolet circular dichroism (CD) spectra were recorded on a Jasco J-40A spectropolarimeter with the samples thermostatted at 25°C. Mean residue weight ellipticities ($[\theta]$) were calculated at each wavelength from 250 to 205 nm, inclusive, after subtracting the solvent blank from each observed ellipticity (θ):

$$[\theta] = \frac{\theta \times 113}{\text{concentration (g/ml)} \times 10 \times \text{path length (cm)}}. \quad (3)$$

Mean residue weight ellipticity, as a function of wavelength, was analyzed with the help of a curve fitting program obtained from Dr. Enrico Bucci (University of Maryland Medical School, Biological Chemistry Department). The program used the basic method of Chen et al. [28] to calculate the most probable fractions of α-helical and β-secondary structure implied by a CD spectrum.

2.5. Radiationless energy transfer

Quenching of Trp-15 by nitrotyrosine-99, nitrotyrosine-138 and by both was measured by comparing the i_∞ of complexes containing a derivatized calmodulin with that of the complex containing native calmodulin and δ-hemolysin. Such comparisons of i_∞ were used to define transfer efficiency:

$$E = 1 - (i_\infty(\text{derivatized})/i_\infty(\text{native})) \quad (4)$$

The inverse sixth power of the separation between donor and acceptor groups is directly related to transfer efficiency

$$E = \frac{R^{-6}}{R_0^{-6} + R^{-6}} \quad (5)$$

and R_0, the critical distance for 50% transfer efficiency, may be calculated from the following relationship [29]:

$$R_0 = \left\{8.79 \times 10^{-5} \times JK^2\phi_0 n^{-4}\right\}^{1/6} \quad (6)$$

In the above relationship J represents the overlap integral between acceptor absorption and donor emission, K^2 an orientation factor, ϕ_0 the donor quantum yield in the absence of acceptor, and n the refractive index of the medium. The overlap integral, J, is given by

$$J = \frac{\int F(\lambda)\epsilon(\lambda)\lambda^4 \, d\lambda}{\int F(\lambda) \, d\lambda} \quad (7)$$

where $F(\lambda)$ is the fluorescence intensity of the donor at wavelength λ and $\epsilon(\lambda)$ the extinction coefficient of the acceptor at the same wavelength. The numerical values of J were computed by trapezoidal integration, using a program written for the Apple II, and data from Cary absorption spectra and Jasco XP-4 emission spectra. The quantum yield (ϕ_0) was obtained from integrals of the spectral distributions of fluorescence of δ-hemolysin and tryptophan. After plotting of graph's, these curves were digitized and integrated using a Hewlett-Packard 9874A digitizer and 9851A calculator. The ratio of areas for samples of equal

concentration was 0.9756 which, when multiplied by 0.14, the assumed quantum yield of tryptophan, gave $\phi_0 = 0.14$, the value used in our calculations [22]. The refractive index of the buffer used in these experiments, 50 mM Mops (pH 6.5) containing 10 mM $CaCl_2$, measured 1.3335 on a Bausch and Lomb refractometer. The problem of assigning a value to K^2 has been discussed elsewhere [25,29] K^2 was taken to be 2/3 here because of the rotational mobility of tyrosine in calmodulin and in calmodulin's aminotyrosine derivatives [22,30].

2.6. Dynamic fluorescence

The fluorescence dynamics of δ-hemolysin and the effect of calmodulin on these properties were measured by time-domain nanosecond fluorometry. The single-photon-counting dynamic fluorometer located at the Regional Laser Biotechnology Laboratory (University of Pennsylvania) was used with the help of Dr. Gary Holtom. Briefly, the system consisted of a mode-locked argon laser driving a rhodamine dye laser that was frequency-doubled and used to excite the sample at a frequency of 3 MHz with 300 nm light. There were monochromators in both the excitation and emission paths; fluorescence was measured at 340 nm. The multichannel analyzer was controlled by a diode downstream from the frequency doubler, and the data acquisition, manipulation and analysis programs were the kind gift of Dr. Holtom.

The excitation beam was vertically polarized and the time decays of the vertically and horizontally polarized components of the fluorescence intensity were monitored. The total intensity $S(t)$ is given by

$$S(t) = \mathrm{VV} + 2\mathrm{VH} \tag{8}$$

where VV and VH are the respective time-dependent intensities of the vertically and horizontally polarized components of the emission intensity excited by vertically polarized light. The instrument response function, which describes the time profile of the excitation pulse, was monitored using a ludox scattering suspension.

The time decay of fluorescence intensity, $S(t)$ was represented as a function of time, t, by:

$$S(T) = \sum_i \alpha_i e^{-t/\tau_i} \tag{9}$$

where α_i and τ_i are the amplitude and decay time, respectively, corresponding to the i-th decay mode. Trial values of the α_i and τ_i were used to generate a trial version of $S(t)$ as a function of time. This was convolved with the instrument response function to generate a computed intensity decay function, $S_c(t)$. This was compared with the experimental decay function, $S_e(t)$, and a value of χ^2 was computed. χ^2, the criterion for goodness of fit, is given by

$$\chi^2 = \sum_j \frac{\{S_e(j) - S_c(j)\}^2}{\rho(j)} \tag{10}$$

where $S_e(j)$ and $S_c(j)$ are the values of $S_e(t)$ and $S_c(t)$, respectively, for the j-th data point and $\rho(j)$ the corresponding precision. For intensity decay data, $\rho(j)$ is equal to $\sqrt{Y(j)}$, where $Y(j)$ is the number of single photon counts for the j-th point.

The set of values of the τ_i which correspond to a minimum value of χ^2 are located by an iterative procedure in which each τ_i is varied in turn until χ^2 passes through a minimum. For each set of values of the τ_i the optimum values of the α_i are identified by a linear least-squares fit.

The time-dependent fluorescence anisotropy, $A(t)$, for vertically polarized excitation, is defined by:

$$A(t) = \frac{\mathrm{VV} - g\mathrm{VH}}{\mathrm{VV} + 2g\mathrm{VH}} \tag{11}$$

where g is given by

$$g = \mathrm{HV}/\mathrm{HH} \tag{12}$$

Here, HV and HH are the vertically and horizontally polarized components of fluorescence excited by horizontally polarized light.

The time decay of anisotropy is represented by a function of the form:

$$A(t) = \sum_i \beta_i e^{-t/\alpha_i} + A(\infty) \tag{13}$$

where the β_i and σ_i are the amplitude and rotational correlation time, respectively, corresponding to the i-th rotational mode and $A(\infty)$ the limiting value of the anisotropy at very long times after excitation.

For vertically polarized excitation, the anisotropy is related to the vertically and horizontally polarized components of fluorescence intensity by:

$$VH = (S/3)(1 - A) \quad (14)$$

$$VV = (S/3)(1 + 2A)$$

In the iterative procedures employed here, the β_i and σ_i are varied so as to minimize simultaneously χ^2 for both VV and VH.

For freely rotating small proteins, it would be expected that $A(\infty)$ should be equal to zero. For free and complexed δ-hemolysin, fits were compared for which $A(\infty)$ was set equal to zero and also for which it was treated as a variable. Little difference was observed in the computed parameters.

3. Results

3.1. Static tryptophan fluorescence

The maximum wavelength (λ_{max}) for emission of free δ-hemolysin is blue-shifted relative to that of tryptophan (334 ± 1 nm vs. 350 nm) (fig. 1). Titration of δ-hemolysin with calmodulin and analysis of the results according to eqs. 1 and 2 yields the values of i_∞ and K_A cited in table 1. It should be stressed that the values of K_A are only apparent and probably correspond to lower limits, since they were computed without regard for the competitive self-association of δ-hemolysin.

The interaction of calmodulin and δ-hemolysin is Ca^{2+}-dependent. In the presence of excess EGTA, the calmodulin-induced fluorescence enhancement is almost abolished (fig. 1).

For the levels of δ-hemolysin employed here (1–3 μM), the emission λ_{max} (334 ± 1 nm) is significantly blue-shifted from the values cited by Cox et al. [17] in the presence of 4 M urea. This presumably is a consequence of the dissociating effect of urea, which results in a displacement of the monomer-polymer equilibria so as to favor monomer and hence exposure of tryptophan to solvent. For our solvent system, which does not contain urea, the presence of excess calmodulin actually causes a slight red shift of λ_{max} to 338 ± 1 nm.

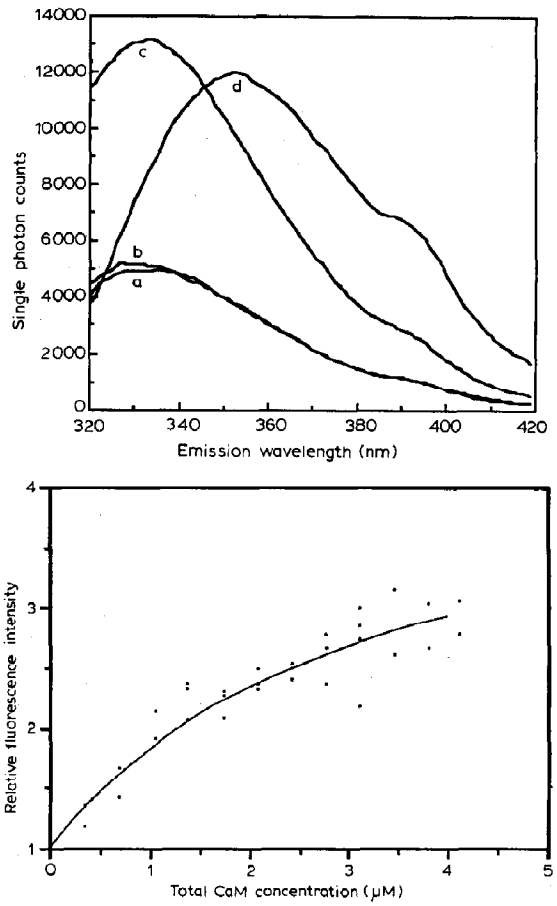

Fig. 1. (Upper) Effect of calmodulin on δ-hemolysin's tryptophan fluorescence. Corrected spectra were obtained on an SLM-8000 system using 280 nm, vertically polarized excitation and single-photon counting of emission polarized at 55°. Background (appropriate buffer in same cuvette) was subtracted and each spectrum displayed is the resultant from two smoothing passes on a raw net data spectrum. (A) 3.0 μM δ-hemolysin in 50 mM Tris (pH 8.0) containing 10 mM EGTA; (B) A plus 4.0 μM calmodulin; (C) B with excess (20 mM) $CaCl_2$; (D) 3.0 μM tryptophan in same buffer as A. (Lower) Fluorimetric titration of δ-hemolysin with calmodulin at pH 8.0. The excitation and emission wavelengths were 305 and 341 nm, respectively. Other conditions were as given in table 1.

Table 1

Overlapping titrations

Buffer	2.02 ml of 50 mM Mops (pH 6.5) containing 20 mM $CaCl_2$	2.02 ml of 50 mM Tris (pH 8.0) containing 20 mM $CaCl_2$
δ-Hemolysin aliquot (nmol)	2.176	2.687
Calmodulin aliquots (nmol)	1.056	0.699
No of runs	3	6
Steps in run	1. 0, 1, 2, 3, 4 2. 0, 4, 5, 6, 7, 8 3. 0, 8, 9, 10, 11, 12	1. 0, 1, 2, 3, 4, 5 2. 0, 3, 4, 5, 6, 7 3. 0, 4, 5, 6, 7, 8, 9 4. 0, 6, 7, 8, 9 5. 0, 8, 9, 10, 11, 12 6. 0, 1, 2, 9, 10, 11, 12
i_∞	2.66	3.23
95% confidence interval	(2.58, 2.74)	(3.13, 3.33)
K_A (M^{-1})	6.85×10^6)	3.81×10^6
95% confidence interval	(2.26×10^6, 9.44×10^6)	(1.71×10^6, 5.90×10^6)

Troponin C and several calmodulin fragments (TM_1, TR_1C, TR_2C) were used to evaluate the role of the gross structural features of calmodulin in the interaction with δ-hemolysin. The tryptic fragments of calmodulin, TR_1C (residues 1–77) and TR_2C (residues 78–148), retain the structural integrity of calmodulin's globular domains. TM_1, the 1–107 fragment resulting from thrombin digestion of calmodulin, and troponin C are species with the central helix (residues 65–92) of calmodulin, or a homologue of it (in troponin C) intact. Table 2 shows the results of experiments in which the effects of these species on δ-hemolysin fluorescence intensity were investigated. Troponin C was the only species, apart from calmodulin itself, which produced a major enhancement of fluorescence.

The data in table 2 show that the structural integrity of calmodulin is a prerequisite for the detection of strong enhancement of δ-hemolysin fluorescence in this system. The long central α-helix of calmodulin, which is intact in TM_1 and represented as a slightly longer homologue in troponin C, is apparently necessary, but not sufficient, for the interaction. Likewise necessary, but not sufficient, is the C-terminal half of the C-terminal globular domain (present in TR_2C, absent from TM_1).

Table 2

Effects of molecular species structurally related to calmodulin on the fluorescence of δ-hemolysin, tested at 1:1 stoichiometry

Excitation and emission wavelengths were 295 and 338 nm, respectively.

Species	[δ-Hemolysin] (μM)	Increase in fluorescence (%)
Calmodulin	1.3	124.7
Troponin C	1.2	88
TM_1	1.2	0
TR_1C	1.3	14
TR_2C	1.3	13

Table 3

Distances between Trp-15 of δ-hemolysin and calmodulin's tyrosine residues implied by radiationless energy transfer in the δ-hemolysin–calmodulin complex

Tyr-199, 0.90 ± 0.18 NO_2 Tyr groups per molecule; Tyr-138, 1.00 ± 0.12 NO_2 Tyr groups per molecule.

Position of nitrotyrosine	R_0 (Å)	R (Å)
Tyr-99	21.7	20.8
Tyr-138	21.1	20.3

3.2. Radiationless energy transfer

To map the interaction site(s) further, radiationless energy transfer from tryptophan to nitrotyrosine was measured. Calmodulin's tyrosine residues (Tyr-99 and Tyr-138) were evaluated for radiationless energy-transfer efficiency from Trp-15 of δ-hemolysin after independent and simultaneous nitration. With nitrotyrosine at both locations the energy-transfer efficiency was 81%. The value of the transfer efficiency to nitrotyrosine-99 alone was 57% and that to nitrotyrosine-138 alone was 56%. From the observed relative quantum yield, the computed spectral overlap integrals, the above transfer efficiencies and the assumptions outlined in section 2, the quantities in table 3 were computed. The observed transfer efficiency to the doubly nitrated calmodulin (81%) agrees within experimental error with the value predicted assuming additivity of the transfer efficiencies to the two nitrotyrosines and thus is consistent with the separations cited above. The measured separations are consistent with a model of the calmodulin–δ-hemolysin interaction in which the central helix and the C-terminal globular domain simultaneously contact δ-hemolysin.

3.3. Acrylamide quenching

The Stern-Volmer constants for dynamic quenching (fig. 2) of δ-hemolysin fluorescence by acrylamide in the absence and presence of calmodulin are, respectively, 7.29 and 2.52. Dividing each of these by the appropriate average fluorescence lifetime leads to the following approximate second-order rate constants for quenching: 5.6×10^9 M^{-1} s^{-1} in the absence of calmodulin and 0.7×10^9 M^{-1} s^{-1} in its presence. Although tryptophan emission of the δ-hemolysin–calmodulin complex is slightly red-shifted relative to that of calmodulin-free δ-hemolysin, the weight of evidence nevertheless shows that the interaction between δ-hemolysin and calmodulin results in the shielding of δ-hemolysin's Trp-15 from the solvent. This result parallels that previously observed for the interaction of melittin and calmodulin, which results in the shielding of Trp-19 of melittin from the solvent [25].

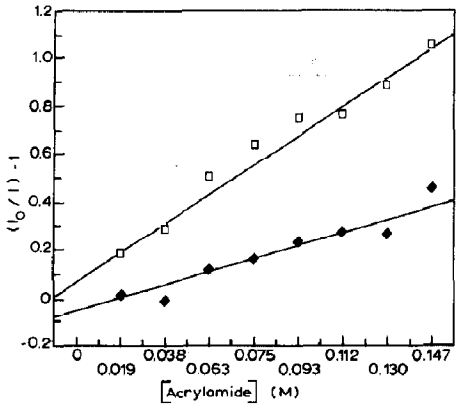

Fig. 2. Acrylamide quenching of δ-hemolysin tryptophan fluorescence in the absence and presence of calmodulin (50 mM Mops, 10 mM $CaCl_2$, pH 6.5). Dynamic quenching: (□) in the absence of calmodulin, slope of fitted line (K_{sv}) is 7.29; (◆) in the presence of calmodulin, slope of fitted line (K_{sv}) is 2.52.

3.4. TNS binding

There is considerable evidence that one of the changes in calmodulin coincident with calcium binding is the formation of an exposed hydrophobic surface [31,32]. Fig. 3 shows the results of a competition experiment between δ-hemolysin and the anionic hydrophobic dye, TNS. TNS (5 μM) was titrated with calmodulin, with δ-hemolysin and with a 1:1 complex of calmodulin and

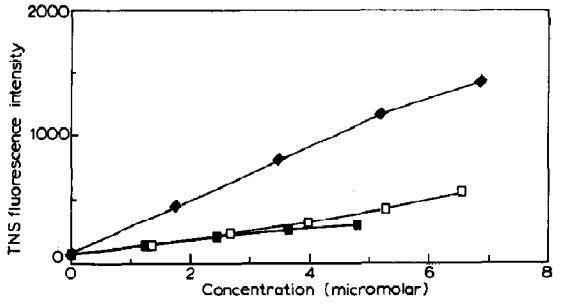

Fig. 3. Competition between-δ-hemolysin and TNS for calmodulin. 5 μM TNS (2.03 ml) in 50 mM Mops (pH 6.5) containing 10 mM $CaCl_2$ was titrated with calmodulin, δ-hemolysin or a 1:1 mixture of calmodulin and δ-hemolysin. Excitation was at 340 nm and emission intensity was measured at 460 nm. Ordinate, net TNS fluorescence; abcissa, total additive concentration. (◆) Calmodulin; (■) δ-hemolysin; (□) complex.

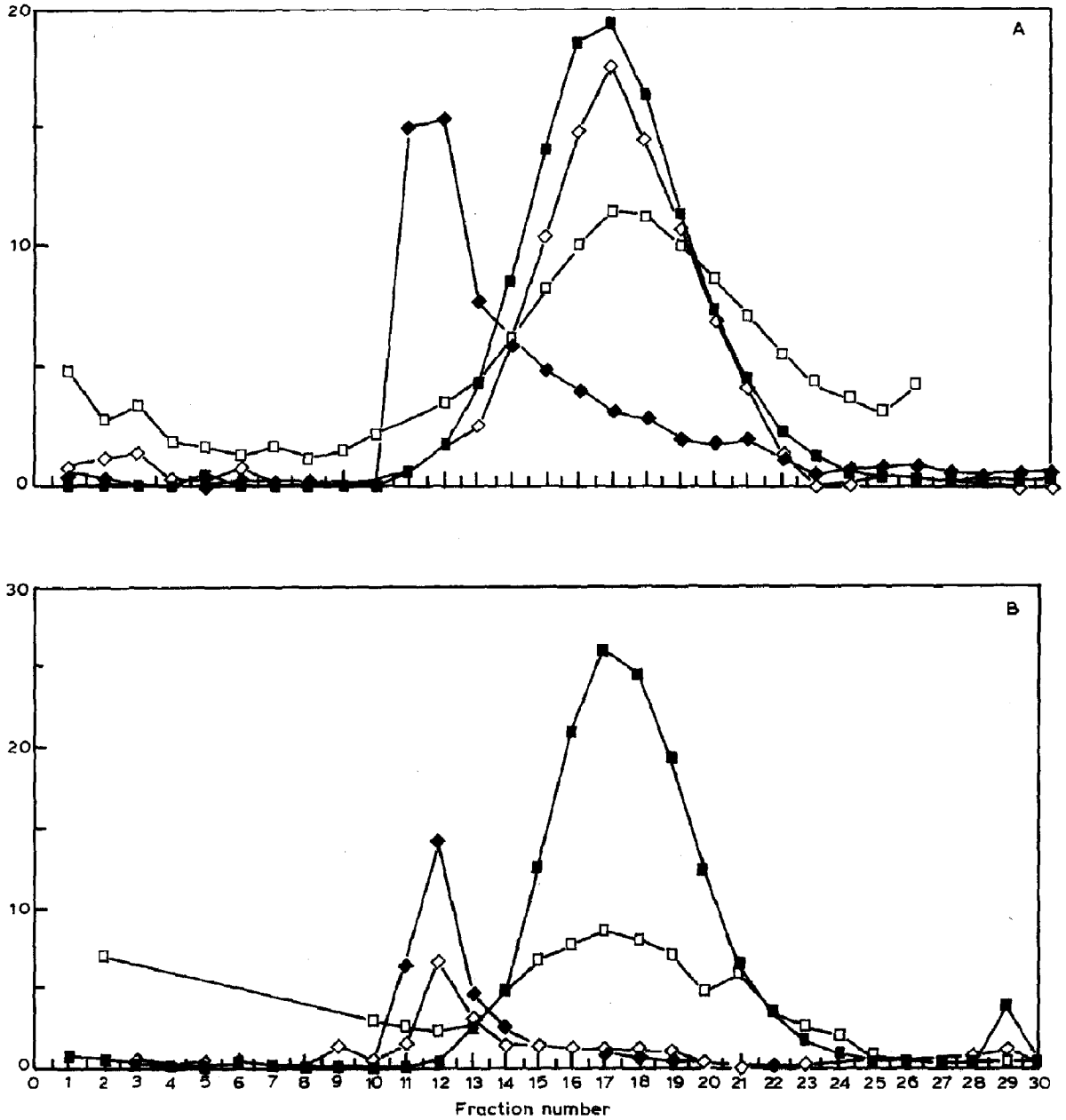

Fig. 4. Gel-filtration chromatography of δ-hemolysin, dinitrocalmodulin and the δ-hemolysin-calmodulin complex. The Sephadex G-100 columns used were 40×1.4 cm (inner diameter) equilibrated in 50 mM Tris (pH 8.0) containing 10 mM $CaCl_2$ or 10 mM EGTA. 1.6-ml fractions were collected. (A) Chromatography in the presence of 10 mM $CaCl_2$. (◆) Net fluorescence of calmodulin-free δ-hemolysin ($\lambda_{ex} = 305$ nm, $\lambda_f = 341$ nm); (□) net A_{230} of dinitrocalmodulin ($\times 10^2$); (◇) net fluorescence of δ-hemolysin applied to column as complex; (■) ^3H cpm of calmodulin applied to column as complex ×1/200. (B) Chromatography in the presence of 10 mM EGTA. (◆) Net fluorescence of calmodulin-free δ-hemolysin; (□) net A_{230} of dinitrocalmodulin ($\times 10^2$); (◇) net fluorescence of δ-hemolysin applied to column as complex; (■) ^3H cpm of calmodulin applied to column as complex (×1/200).

δ-hemolysin, all in the presence of 10 mM $CaCl_2$. Fig. 3 indicates that the effects produced by the two species are not additive and that the complex is less effective than calmodulin alone. The fluorescence titration profile of TNS in the presence of the δ-hemolysin–calmodulin complex is roughly the same as that of TNS plus δ-hemolysin alone; this result suggests that δ-hemolysin competes, successfully, with TNS for a hydrophobic binding site on calmodulin. In this respect, δ-hemolysin stands in contrast to melittin, whose binding by calmodulin enhances the binding of TNS [33].

3.5. Gel filtration

The following gel-filtration experiment provides direct evidence that Ca^{2+}-activated binding of δ-hemolysin by calmodulin is implicated in calmodulin's effects on δ-hemolysin fluorescence. Fig. 4 shows the elution profiles of two 40 × 1.4 cm Sephadex G-100 columns. The difference between panels A and B is that the former depicts gel-filtration chromatography in the presence of 10 mM $CaCl_2$ and the latter represents the same experiment in the presence of 10 mM EGTA. The samples applied to and eluted from both columns were Blue dextran, doubly nitrated calmodulin, pure δ-hemolysin, and the δ-hemolysin–calmodulin complex (1 : 2 mole ratio) in 50 mM Tris (pH 8.0) containing 10 mM $CaCl_2$ (A) or 10 mM EDTA (B). The elution profiles obtained using tryptophan fluorescence and ^3H radioactivity clearly show that δ-hemolysin and tritiated calmodulin migrate as a single species in the presence of $CaCl_2$ but do not do so in the presence of EGTA. This behavior confirms that δ-hemolysin does not bind Ca^{2+}-free calmodulin.

Fig. 4 also indicates that δ-hemolysin alone migrates more rapidly than either calmodulin or the complex, in harmony with expectations if δ-hemolysin exists as self-associated species.

3.6. Trypsin digestion

The susceptibility to proteolysis by trypsin of Ca^{2+}-liganded calmodulin is restricted. The primary site of attack is the link between residues 77 and 78, although secondary points of attack are also present [25]. Since the primary site of proteolysis lies in the center of the connecting strand, it might be expected that the involvement of this structural region in complex formation with a

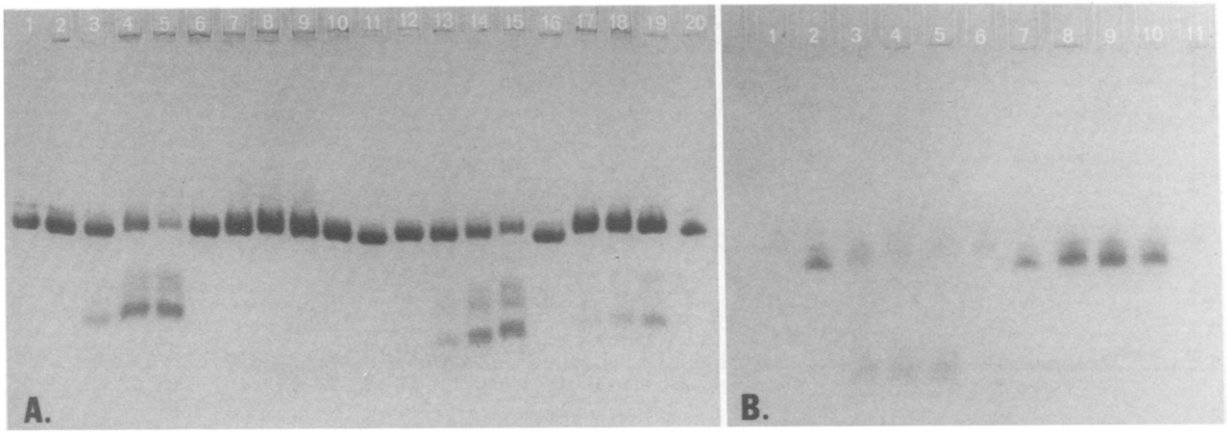

Fig. 5. Effect of complexation with δ-hemolysin on the trypsin sensitivity of calmodulin (see section 2). The gel was 12.5% acrylamide and electrophoresis was conducted in the presence of 4 M urea and 2 mM EGTA at pH 8.8. (A) Time course of trypsin digestion in the absence of δ-hemolysin (lanes 2–5, 54 μM CaM; lanes 12–15, 108 μM CaM), in the presence of equimolar δ-hemolysin (lanes 6–9), and in the presence of 1 : 2 δ-hemolysin–CaM (lanes 16–19). All digestions were made with 0.87 μM trypsin. Calmodulin standard was loaded in lanes 1, 10, 11 and 20. Digestion times for each set of four lanes were 0, 5, 15, and 30 min. (B) Time course of digestion of dinitrocalmodulin (Tyr-99 and Tyr-138 converted to nitrotyrosine) in the absence and presence of equimolar δ-hemolysin. Electrophoresis conditions and trypsin concentration as in panel A. Digestion in the absence of δ-hemolysin (lanes 2–5) and in its presence (lanes 7–10). Digestion times for each set of four lanes were 0, 15, 30, and 60 min.

polypeptide would block proteolytic attack by trypsin. This has proved to be the case for complexes of calmodulin with melittin [18].

In order to examine the possibility that the 1 : 1 complex formed by calmodulin and δ-hemolysin involves the central helix, the time course of trypsin hydrolysis of Ca^{2+}-liganded calmodulin was monitored in the absence and presence of δ-hemolysin by means of urea gel electrophoresis (fig. 5).

The photograph in fig. 5 shows electrophoretic separations of the products of trypsin digestion of calmodulin in the absence and presence of δ-hemolysin. Panel A illustrates the effect of δ-hemolysin on the trypsin sensitivity of native calmodulin and panel B shows those on the trypsin digestion of doubly nitrated calmodulin. In fig. 5A, lanes 2–5 show the time course of the cleavage of native calmodulin (54 μM) and lanes 6–10 depict the complete loss of sensitivity to trypsin in the presence of equimolar δ-hemolysin. Lanes 12–15 show the time course of digestion of 108 μM calmodulin and lanes 16–19 demonstrate that excess calmodulin (108 μM) retains its trypsin sensitivity in the presence of that concentration of δ-hemolysin (54 μM) which fully protected equimolar calmodulin. Fig. 5B shows calmodulin for which both Tyr-99 and Tyr-138 have been modified by reaction with tetranitromethane (dinitrocalmodulin); this species retained both trypsin sensitivity in the absence of δ-hemolysin, and the ability to be protected from trypsin by the interaction with δ-hemolysin.

It thus appears that the 1 : 1 complex of δ-hemolysin with Ca^{2+}-liganded calmodulin resembles the analogous complex formed by melittin in being resistant to the action of trypsin [18].

3.7. Circular dichroism

Melittin, another amphipathic polypeptide which binds to calmodulin, has been found to experience striking changes of secondary structure because of the interaction [3]. To investigate the possibility of similar conformational alterations in the δ-hemolysin–calmodulin interaction, far-ultraviolet CD spectra were recorded and compared with respect to the secondary structure implied by the spectral distributions of mean residue weight ellipticities [28]. The results are displayed in table 4.

Table 4

Computed distributions of secondary structure implicit in CD spectra of δ-hemolysin, calmodulin and δ-hemolysin–calmodulin

The values have been computed according to the theory of ref. 28 and are useful primarily for comparative purposes. $[\theta]_{222}$, mean residue weight ellipticity (in cm^2 degree $dmol^{-1}$ residues).

Species	$[\theta]_{222}$	% α-helix	% β-structure	% random coil
Calmodulin	−17600	52.1±2.0	31.4± 8.1	16.1±10.1
δ-Hemolysin	−26500	87.1±3.1	12.2±12.6	0.4±19.7
δ-Hemolysin–calmodulin	−18400	53.4±2.1	28.4± 8.5	18.2±10.7

An additive model of mean residue weight ellipticity in the complex, i.e., a model assuming zero conformational change in both δ-hemolysin and calmodulin [28], predicts formally the following secondary structure composition: 59.3 ± 5.2% α-helix, 25.0 ± 20.3% β-structure and 15.6 ± 25.7% random coil. The data in table 4 are consistent, within experimental uncertainty, with an additive model of mean residue weight ellipticity in the complex. Unlike the case of melittin, there is no evidence suggesting that a change of secondary structure occurs when δ-hemolysin binds to calmodulin.

3.8. Dynamic fluorescence

In order to examine more closely the question of the mobility of Trp-15, as well as the hydrodynamic characteristics of the 1 : 1 complex, time-domain measurements were performed on the time decay of the intensity and anisotropy of tryptophan fluorescence for free and complexed δ-hemolysin (see section 2). Since tyrosine does not absorb at 300 nm, the excitation wavelength employed here, the results for the complex are not complicated by tyrosine emission.

The time decay of fluorescence intensity was multiexponential for both free δ-hemolysin and the complex (table 5). In both cases an optimal fit required the assumption of three decay components (fig. 6 and table 5). This does not necessarily

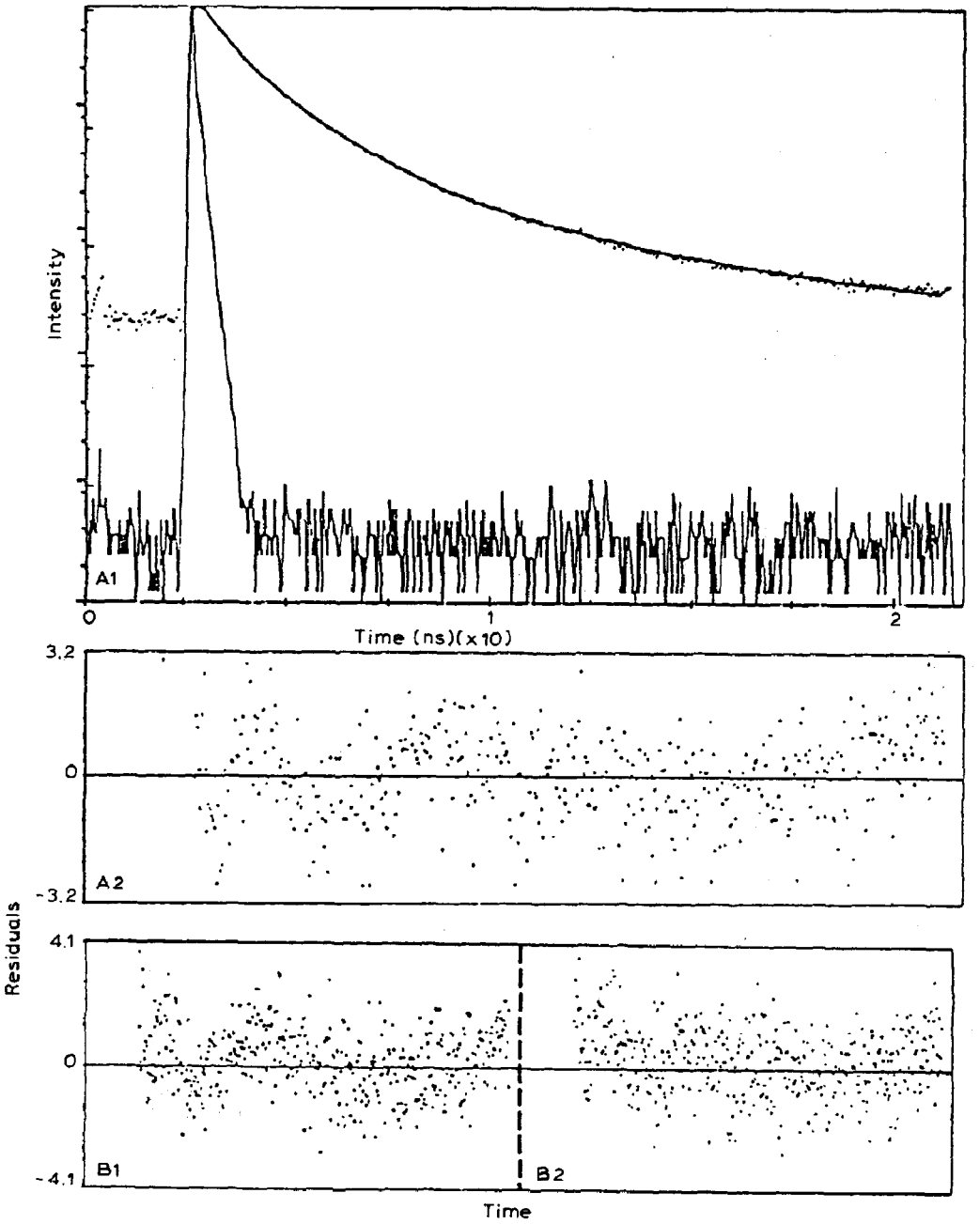

Fig. 6. (Upper) Time decay of emission intensity for δ-hemolysin (upper curve) and the ludox scattering solution (lower curve). (Middle) Distribution of residuals for lifetime fit, assuming three components, for data displayed in upper curve using values cited in table 5. (Lower) Distribution of residuals for vertically (left) and horizontally (right) polarized components of fluorescence using fits obtained with parameters cited in tables 5 and 6 (0.0424 ns/channel).

mean that three discrete components are strictly present. A plausible alternative possibility is that a distribution of decay times exists and that the observed decay times are actually averages. The average decay time increases substantially upon complex formation with calmodulin. This is consistent with expectations in view of the increase in quantum yield; both effects reflect the altered microenvironment of Trp-15.

The time decay of fluorescence anisotropy for free δ-hemolysin was likewise multiexponential, corresponding to a rapid rotational mode of correlation time less than 1 ns and a slow rotational mode of correlation time greater than 30 ns. The amplitudes of the two correlation times are comparable. The magnitude of the shorter correlation time indicates that it reflects a localized motion of the fluorophore involving a limited number of residues (table 6). Its high relative amplitude suggests that Trp-15 has a substantial mobility within the overall structure.

Table 6

Fluorescence anisotropy decay parameters of δ-hemolysin and of the δ-hemolysin–calmodulin complex

Experiment	Time/channel (ns)	β (amplitude)	σ (correlation time) (ns) [a]	χ^2
δ-Hemolysin	0.0424	0.11	0.39	
		0.13	76.32	1.26
			$\bar{\sigma} = 40.98$	
Complex	0.0857	0.02	1.82	
		0.26	11.17	1.18
			$\bar{\sigma} = 10.58$	
δ-Hemolysin	0.0087	0.09	0.40	
		0.17	34.69	1.25
			$\bar{\sigma} = 22.33$	
Complex	0.0087	0.02	0.42	
		0.265	11.14	1.17
			$\bar{\sigma} = 10.31$	

[a] $\bar{\sigma} = \Sigma\beta_i\sigma_i^2/\Sigma\beta_i\sigma_i$.

Table 5

Fluorescence lifetime parameters of δ-hemolysin and of the δ-hemolysin–calmodulin complex

Experiment	Number of components assumed	Time/channel (ns)	α (amplitude)	τ (lifetime) (ns) [a]	χ^2
δ-Hemolysin	3	0.0424	0.30	0.45	
			0.33	1.28	
			0.04	4.48	1.26
				$\bar{\tau} = 1.04$	
1:1 complex	3	0.0875	0.33	0.52	
			0.73	2.76	
			0.27	6.28	1.18
				$\bar{\tau} = 4.21$	
δ-Hemolysin	2	0.0087	0.16	0.48	
			0.13	1.77	1.68
				$\bar{\tau} = 1.44$	
δ-Hemolysin	3	0.0087	0.07	0.12	
			0.17	0.64	
			0.09	2.08	1.22
				$\bar{\tau} = 1.54$	
1:1 complex	2	0.0087	0.03	0.47	
			0.10	3.46	1.17
				$\bar{\tau} = 3.33$	

[a] $\bar{\tau} = \Sigma\alpha_i\tau_i^2/\Sigma\alpha_i\tau_i$.

The magnitude of the longer correlation time is greatly in excess of that expected for monomeric δ-hemolysin and consistent with the presence of large self-associated species, as suggested by the gel-filtration measurements. Its apparent magnitude varies according to the fraction of the decay curve which is analyzed and is smaller when a time per channel of 8.7 ps is selected, restricting the total time of observation to approx. 4 ns, than for a time per channel of 42.4 ps. This is consistent with the presence of a range of correlation times, reflecting heterogeneity of the associated species.

Complex formation with calmodulin results in a substantial suppression of the amplitude of the rapid rotational mode (table 6)), whose contribution now becomes minor, although its magnitude (0.4–1.8 ns) is comparable to that for the free species. The slower rotational mode, which now dominates the anisotropy decay, has a correlation time whose magnitude (11 ns) is similar to that expected for calmodulin itself.

These observations are consistent with the formation of a 1:1 complex by calmodulin and

δ-hemolysin in which Trp-15 is highly immobilized, in harmony with the CD results cited earlier.

4. Discussion

The results presented here are consistent with three conclusions. First, δ-hemolysin and calmodulin interact in the presence of Ca^{2+} with moderately high affinity to form a complex. Second, both the extended connecting helix (residues 65–92) and the C-terminal globular domain of calmodulin are probably involved in the interaction with δ-hemolysin. Third, hydrophobic contacts make a contribution to the stabilization of the complex.

The gel-filtration experiments indicate that, in the presence of excess calmodulin, δ-hemolysin migrates with a mobility similar to that of calmodulin itself and strikingly different from that of free δ-hemolysin. The elution position of the latter is consistent with earlier findings that δ-hemolysin exists in aqueous solution as large aggregates [6,17]. The similarity in mobility of the complex and uncombined calmodulin suggests that the average number of δ-hemolysin molecules combined per calmodulin molecule is not large, but does not establish the stoichiometry. Similar conclusions follow from the similarity of the rotational correlation time of the complex to that expected for native calmodulin. However, the observation that δ-hemolysin in a 1 : 1 mole ratio can block the tryptic hydrolysis of calmodulin is a strong indication that the dominant complex formed under these conditions is 1 : 1 and that the binding of δ-hemolysin aggregates by calmodulin is not an important factor. If the stoichiometry were other than 1 : 1, a significant proportion of free calmodulin would be present, which would be susceptible to trypsin digestion.

The second conclusion, that binding to δ-hemolysin involves two gross structural features of calmodulin, namely, the long central helix and the C-terminal globular domain, rests upon the effects of calmodulin fragments upon the tryptophan fluorescence of δ-hemolysin, the resistance to trypsin hydrolysis conferred by 1 : 1 complex formation with δ-hemolysin, and the measured distances between Trp-15 and the tyrosines of calmodulin. None of the above evidence is conclusive in itself. For example, it is conceivable that the TM_1 (1–106) fragment of calmodulin might combine with δ-hemolysin without modifying its tryptophan fluorescence, while the resistance to trypsin digestion of the complex might arise indirectly from an induced structural change. Nevertheless, the simplest model consistent with all the above observations is that cited above, which postulates the involvement of both the central helix and the C-terminal zone of calmodulin in the interaction.

With respect to the third conclusion, the formulation of a hydrophobic patch or trough by the C-terminal half of Ca^{2+}-liganded calmodulin was predicted by early solution studies and established conclusively by X-ray crystallography [31,35–37]. This hydrophobic region, which includes side chains of both the C-terminal lobe and the central helix, is a plausible location for a binding site of TNS and, by implication, a potential zone of contact for δ-hemolysin. (Follenius and Gerard [38] have shown that binding sites for TNS occur on both halves of calmodulin). It is of interest that the completely α-helical δ-hemolysin monomer would be approx. 40 Å length. This is sufficiently long to permit extensive contact with both the central helix and the C-terminal lobe and perhaps the N-terminal lobe as well.

δ-Hemolysin differs from the other toxic polypeptides, such as melittin, which form stable complexes with Ca^{2+}-liganded calmodulin in that it appears to exist even at low ionic strengths as amphipathic helices which interact to form large aggregates. The α-helical structure persists in the complexes formed with calmodulin.

The red-shifted character of the tryptophan fluorescence of free δ-hemolysin suggests a relatively nonpolar environment, while the high rotational mobility and accessibility to quencher are consistent with some degree of exposure to solvent. It is possible that, in the aggregates, Trp-15 may lie on the edge of a hydrophobic face and thereby exist in a partially nonpolar microenvironment without being incorporated into a rigid structure [12,39]. When δ-hemolysin is combined with calmodulin in a 1 : 1 complex, Trp-15 behaves as if imbedded in the zone of contact so as to be solvent-shielded and immobilized.

References

1 R.E.O. Williams and G.H. Harper, J. Pathol. Bacteriol. 59 (1947) 69.
2 A. Yoshida, Biochim. Biophys. Acta 71 (1963) 544.
3 N.G. Heatley, J. Gen. Microbiol. 69 (1971) 269.
4 F.S. Nolte and F.A. Kapral, ASM Annual Meeting, Abstr. 812 (1979).
5 J.E. Fitton, A. Dell and W.V. Shaw, FEBS Lett. 118 (1980) 209.
6 H.S. Kantor, B. Temples and W.V. Shaw, Arch. Biochem. Biophys. 151 (1972) 142.
7 G. Colacicco, M.K. Basu, A.R. Buckelew, Jr and A.W. Bernheimer, Biochim. Biophys. Acta 465 (1977) 378.
8 J.E. Fitton, FEBS Lett. 130 (1981) 257.
9 J.E. Fitton, D.F. Hunt, J. Marasco, J. Shabanawity, S. Winston and A. Dell, FEBS Lett. 169 (1984) 25.
10 M. Schiffer and A.B. Edmondson, Biophys. J. 7 (1967) 121.
11 E.T. Kaiser and F.J. Kezdy, Science 223 (1984) 249.
12 J.H. Freer and T.H. Birkbeck, J. Theor. Biol. 94 (1982) 535.
13 J.H. Wang, C.J. Pallen, R.K. Sharma, A. Adachi and K. Adachi, Curr. Top. Cell Regul. 27 (1985) 419.
14 D.A. Malencik and S.R. Anderson, Biochemistry 22 (1983) 1995.
15 D.A. Malencik and S.R. Anderson, Biochemistry 23 (1984) 2420.
16 S.R. Anderson and D.A. Malencik, in: Calcium and cell function VI, ed. W.Y. Cheung (Academic Press, New York, 1986) p. 1.
17 J.A. Cox, M. Comte, J.E. Fitton and W.F. DeGrado, J. Biol. Chem. 260 (1985) 2527.
18 C.G. Caday and R.F. Steiner, Biochem. Biophys. Res. Commun. 135 (1986) 419.
19 R. Gopalakrishna and W.B. Anderson, Biochem. Biophys. Res. Commun. 104 (1982) 830.
20 D.W. Watterson, W.G. Harrelson, Jr, P.M. Keller, F. Sharief and T.C. Vanaman, J. Biol. Chem. 251 (1976) 4501.
21 N. Jentoft and D.G. Dearborn, J. Biol. Chem. 254 (1979) 4359.
22 R.F. Steiner and L. Marshall, Biopolymers 24 (1985) 547.
23 D.L. Newton, M.D. Oldewurtel, M.H. Krinks, J. Shiloach and C.B. Klee, J. Biol. Chem. 259 (1984) 4419.
24 D.M. Watterson, F. Sharief and T.C. Vanaman, J. Biol. Chem. 255 (1980) 962.
25 R.F. Steiner, L. Marshall and D. Needleman, Arch. Biochem. Biophys. 246 (1986) 286.
26 C.R. Cantor and P.R. Schimmel, Biophysical Chemistry (W. Freeman, San Francisco, 1980) ch. 8.
27 D.B. Calhoun, J.M. Vanderkooi and S.W. Englander, Biochemistry 22 (1983) 1533.
28 Y. Chen, J.T. Yang and K.H. Chau, Biochemistry 13 (1974) 3350.
29 R.H. Fairclough and C.R. Cantor, Methods Enzymol. 48 (1978) 347.
30 P.K. Lambooy, R.F. Steiner and H. Sternberg, Arch. Biochem. Biophys. 217 (1982) 517.
31 T. Tanaka and H. Hidaka, J. Biol. Chem. 255 (1980) 11078.
32 D.C. LaPorte, B.M. Wierman and D.R. Storm, Biochemistry 19 (1980) 3814.
33 R.F. Steiner and L. Norris, Biophys. Chem. 27 (1987) 27.
34 Y. Maulet and J.A. Cox, Biochemistry 22 (1983) 5680.
35 J. Gariepy and R.S. Hodges, Biochemistry 22 (1983) 1586.
36 J.F. Head, H.R. Masure and B. Kaminer, FEBS Lett. 137 (1982) 71.
37 Y.S. Babu, J.S. Sack, T.G. Greenhough, C.E. Bugg, A.R. Means and W.J. Cook, Nature 315 (1985) 37.
38 A. Follenius and D. Gerard, Biochem. Biophys. Res. Commun. 119 (1984) 1154.
39 C. Cohen and D.A.D. Parry, Trends Biol. Sci. June '86 (1986) 245.